Int J Adv Manuf Technol (2017) 92:3871–3882
DOI 10.1007/s00170-017-0425-8

ORIGINAL ARTICLE

Multiphysics modelling and experimental investigations of the filling and curing phases of bi-injection moulding of thermoplastic polymer/liquid silicone rubbers

H. Ou[1] · **M. Sahli**[1] · **T. Barrière**[1,2] · **J. C. Gelin**[1]

Received: 4 September 2016 / Accepted: 12 April 2017 / Published online: 5 May 2017

Abstract Liquid silicone rubber (LSR) is a family of high-technology elastomer materials. The member of this family has been identified as being very promising for development in the coming decades due to their unique properties and ease of generation in large series by the injection moulding process. In particular, the over-moulding of LSR on other materials, such as thermoplastic polymers, metals and ceramics, is possible today, which leads to the possibility of obtaining multi-material, functional multi-colour and newly featured components. The work presented in this paper focuses on the transformation of liquid silicone rubber to better understand the phenomena involved to improve production processes and to optimize the processing conditions for bi-material components in well-defined geometry and functional properties. The rheological, rheo-kinetic and thermal behaviours of silicone elastomers were investigated and characterized under real conditions of manufacture with different combined methods. A thermo-rheo-kinetic model was then developed and implemented using the moulding simulation software Cadmould® 3D to simulate two-component injection moulding of silicone rubber into a thermoplastic polymer. For the validation of the models chosen and the parameters identified, bi-material injection moulding tests of a two-component standard peel test specimen (polyamide thermoplastic polymer/liquid silicone rubber) were performed and compared to numerical results.

✉ T. Barrière
thierry.barriere@ens2m.fr

[1] Applied Mechanics Department, FEMTO-ST Institute, 24 Rue de l'Epitaphe, 25000 Besançon, France

[2] Department of Applied Mechanics, COMUE UBFC, FEMTO-ST Institute, University Bourgogne-Franche-Comté, 24 Rue de l'Epitaphe, 25030 Besançon, France

Keywords Liquid silicone rubber · Polyamide thermoplastic polymer · Bi-material injection moulding · Physical characterization · Thermo-rheo-kinetic model · Numerical simulation

1 Introduction

Silicone elastomer is a specific thermosetting elastomer material that consists of an inorganic silicon-oxygen backbone chain with organic groups attached to silicon atoms. Silicone elastomers could be divided into three groups depending on their rheological and kinetic properties: high consistency rubber (HCR), room-temperature vulcanising (RTV) and liquid silicone rubber (LSR) [1]. Otherwise, liquid silicone rubbers are identified as having the strongest arguments for development in the coming decades due to their unique properties and ease of formation by the injection moulding process, which is the most common and most cost-effective process for making plastic products that have intricate shapes in high-volume production due to its high efficiency and manufacturability. As a result, silicone rubber presents the characteristics of both inorganic and organic materials. It offers many advantages and specific properties over traditional materials, such as low toxicity, excellent weatherability and good thermal stability; mechanical properties such as superior chemical resistance; and electrical insulation properties, as well as biodurability and biocompatibility with specific architecture materials with NiTi silicone composites [2–4]. LSR is a versatile material and is preferred over other polymers, especially in medical applications, due to its biocompatibility, heat resistance, flexibility and self-lubrication [5]. It is also used widely in automotive, electrical and consumer products [6].

The LSR injection moulding process is very similar to the conventional thermoplastic injection moulding process, but

there is a major difference in the solidification phase. During thermoplastic injection moulding, the injected materials are heated and melted by an injection screw and then filled into a mould cavity. Rapid cycling is obtained during the injection, packing, cooling and ejection phases of the process [7].

In contrast, two-part liquid silicone rubber materials are metered and mixed by a specific dosing system and then injected cold into a preheated die cavity mould, where the mixture of LSR is solidified exothermally by a chemical cross-linking reaction called "curing" [8]. The curing of LSR is generally carried out with a platinum-catalysed hydrosilylation reaction and necessitates a relatively long solidification time in comparison to the injection cycle time. Some new types of curing systems have been developed to obtain very excellent mechanical properties [9]. Some studies have focused on possible degradation mechanisms due to the addition of specific curing constituents [10]. In addition, the physical and mechanical properties of silicone rubber are significantly affected by the kinetic curing behaviour [11]. Thus, the rheo-kinetic models for elastomer silicones, such as the curing temperature and the curing time, are very important for the optimization of the LSR injection moulding process and the achievement of final silicone rubber components [12]. Different experimental methods have been developed to measure the different stages of the curing phase [13].

With the progress made in material innovation and process technology, multi-component injection moulding has been largely developed and used in industry. It offers a large number of possibilities for obtaining multi-colour parts, multi-material parts and parts that have novel functionality to satisfy the growing demands in the fields of safety, ergonomics and aesthetics, among others. The plastic injection over-moulding process is an important technique within multi-component injection moulding, which is one of the most common transformation processes used to combine two different materials, such as a thermoplastic polymer and liquid silicone rubber, in a single part [14]. During the over-moulding process, an elastomer material is moulded over or around a compatible substrate (typically, a rigid plastic) by using insert moulding or multi-shot injection moulding processes [15]. The quality of the multi-components obtained strongly depends on the interfacial adhesion strength [16]. However, there are a large number of parameters that influence the adhesion strength between two materials, including the preparation of the substrate surface, the chemical composition of the liquid silicone rubber material and the thermal history during the curing process [17]. Therefore, even the description of the mechanism of adhesion in simple terms is complex due to the various related phenomena involved.

Process parameters play an important role in plastic injection moulding as they influence the quality of the moulded part and also affect the productivity, cycle time and energy consumption of the moulding process [18]. However, the optimization of moulds and process parameters for thermoplastic injection moulding by the trial-and-error method in a series of moulding tests is both expensive and time consuming [19]. Currently, with the development of computer technology, computer-aided engineering simulation tools have been successfully used in the prediction and optimization of the thermoplastic injection moulding process without physically committing real material and machine time [20]. The simulation of conventional injection moulding as well as complex injection moulding processes, such as gas assist, co-injection, over-moulding and sequential moulding, has become a common place. This is unfortunately not true in the case of the LSR moulding process [21].

This paper includes modelling and is focused on research related to the simulation of the liquid silicone rubber injection moulding process applied to two-material components with thermoplastic polymer and liquid silicone rubber. The thermo-rheo-kinetic model coupling the heat transfer and the rheological and curing kinetic behaviours during injection moulding have been taken into account and implemented in moulding using finite element Cadmould® software.

For determining and identifying the parameters of the thermo-rheo-kinetic model of different liquid silicone rubber materials, rheological measurements and kinetic characterization were achieved by using a rotational rheometer. The experimental rheological results were fitted by a Carreau-Yasuda model with the temperature dependence characterized by the Williams-Landel-Ferry (WLF) equation. The evolution of the cure reaction kinetics was described by the Isayev-Deng model using the inverse method. In addition, the thermo-physical properties of silicone liquid rubbers, such as the density, specific heat and thermal conductivity, were also measured under real industrial conditions. To validate the proposed model and the identified parameters, finite element simulation of the filling process results was compared to moulding tests performed on a polyamide thermoplastic polymer/liquid silicone rubber to evaluate a standard peel test specimen without defects.

2 Rheo-kinetic models and method of specific identification

2.1 Viscosity model

Various models exist to describe the evolution of shear viscosity with the temperature and shear rate for polymer materials. However, the accuracy of numerical simulation is critically dependent on the ability of the various rheological models to predict the material flow over the range of shear rates,

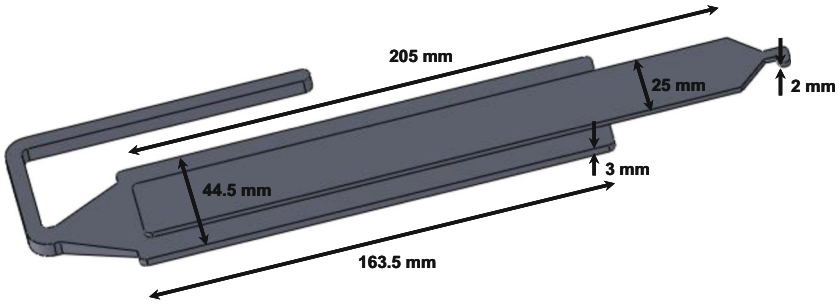

Fig. 1 Geometries of the PA 66/LSR standard peel test specimen

temperatures and pressures encountered during the injection moulding process. In this study, the Carreau-Yasuda model was chosen [22].

$$\eta(\dot{\gamma}, T) = \eta_0(T)\left(1 + \left(\frac{\eta_0(T)\dot{\gamma}}{\tau}\right)^{A}\right)^{\frac{n-1}{A}} \quad (1)$$

where η_0, τ, a and n are the fitting parameters. More specifically, η is the shear viscosity (Pa·s), η_0 is the apparent shear viscosity at zero shear rate (Pa·s), $\dot{\gamma}$ is the shear rate (s^{-1}), T is the temperature (K), τ represents the critical shear stress roughly characterizing the transition shear stress from the Newtonian range to the shear-thinning region, A determines the width of the transition region and n is the power law index describing the slope of the viscosity curve with respect to the shear rate in the shear-thinning region. For a shear-thinning fluid, n is between 0 and 1, and for a shear-thickening fluid, it is greater than 1. The flow behaviour index of the power law index indicates shear sensitivity. A thermoplastic polymer with a smaller n value indicates that the polymer has higher shear sensitivity and more pseudoplasticity. Some moulding defects are associated with small values of n, i.e., higher shear sensitivity. The parameters η_0 and n influence the transition between the shear threshold at a low shear rate and the portion of the curve following a power law behaviour. In the simulation software, A was chosen to be equal 1.

The temperature dependence is calculated according to the WLF equation [23]. The WLF equation has the following form:

$$\log(a_T) = \log\left(\frac{\eta_0(T)}{\eta_0(T_0)}\right) = -\frac{C_1(T-T_0)}{C_2 + (T-T_0)} \quad (2)$$

where T_0 is the reference temperature chosen to construct the compliance master curve and C_1 and C_2 are empirical constants that are adjusted to fit the values of the superposition parameter a_T. C_1 and C_2 are positive constants that depend on the material and the reference temperature. The principle of time temperature superposition states that the change in temperature from T to T_0 is equivalent to multiplying the time scale by the constant factor a_T which is only a function of the two temperatures (T to T_0). The quantity a_T is called "horizontal translation factor" or the shift factor and has the properties: $T > T_0 \rightarrow a_T > 1$, $T < T_0 \rightarrow a_T < 1$ and $T = T_0 \rightarrow a_T = 1$.

2.2 Kinetic modelling

From such different methods, a parameter known as the cure degree is defined and plotted versus time to give a useful representation describing the temporal behaviour of the curing reaction and describing chemical reactions that occur during the curing process [24]. There are two types of system models that have been developed in the literature, namely mechanistic kinetic models and phenomenological [25] or empirical models [26]. The cure degree quantifies the balance of the chemical species involved in reactions to form the mathematical relationships connecting the reaction rate path to the cure time and temperature. Many kinetic models have been developed to describe the cure behaviour, especially the model of Kamal and Sourour [28] and Isayev and Deng [29]. The kinetic cure parameters were defined using the proposed models of Claxton and Liska [27] and Isayev and Deng [29], which are frequently used for kinetic curing modelling applied to elastomers.

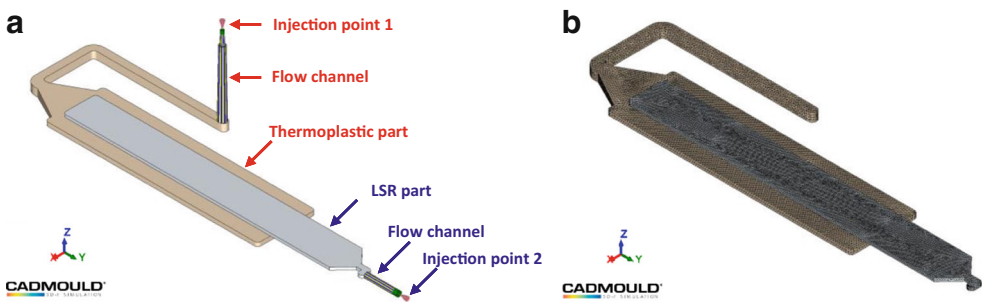

Fig. 2 **a** Illustration of PA 66/LSR injection moulding. **b** The finite element meshes of the bi-material standard peel test specimen

Table 1 Process parameters used in the simulation for polyamide PA 66/LSR injection moulding

Process parameters	Injection parameters for polyamide substrate (PA 66)	Injection parameter for over-moulding LSR on polyamide substrate (PA 66)
Melt temperature (°C)	245	20
Mould temperature (°C)	80	180
Flow rate ($cm^3\ s^{-1}$)	25	2
Packing pressure (MPa)	35	11
Packing time (s)	10	1.2
Cooling time (s)	60	–
Heating time (s)	–	60

From the cure data obtained from the rheometer [29], the cure degree (α) can be calculated using the following equation:

$$\alpha = \frac{G'(t) - G'_{\min}}{G'_{\max} - G'_{\min}} \tag{3}$$

where $G'(t)$, $G'_{\max}$ and $G'_{\min}$ are the elastic modulus at time t, the maximum elastic modulus and the minimum elastic modulus during the curing reaction, respectively. The state of a rubber during an isothermal vulcanization reaction can be described by a cure degree (α) ranging from 0 (uncured) to 1 (complete reaction) [30]. The raw data obtained is complex torque M^*, the real part of which G' is related to the storage modulus of the rubber. This degree of cure is generally obtained from dynamic rheological measurements of elastic modulus (G'), initially equal to $G'_{\min}$ [30]. Three steps are generally observed: an induction period, during which the modulus

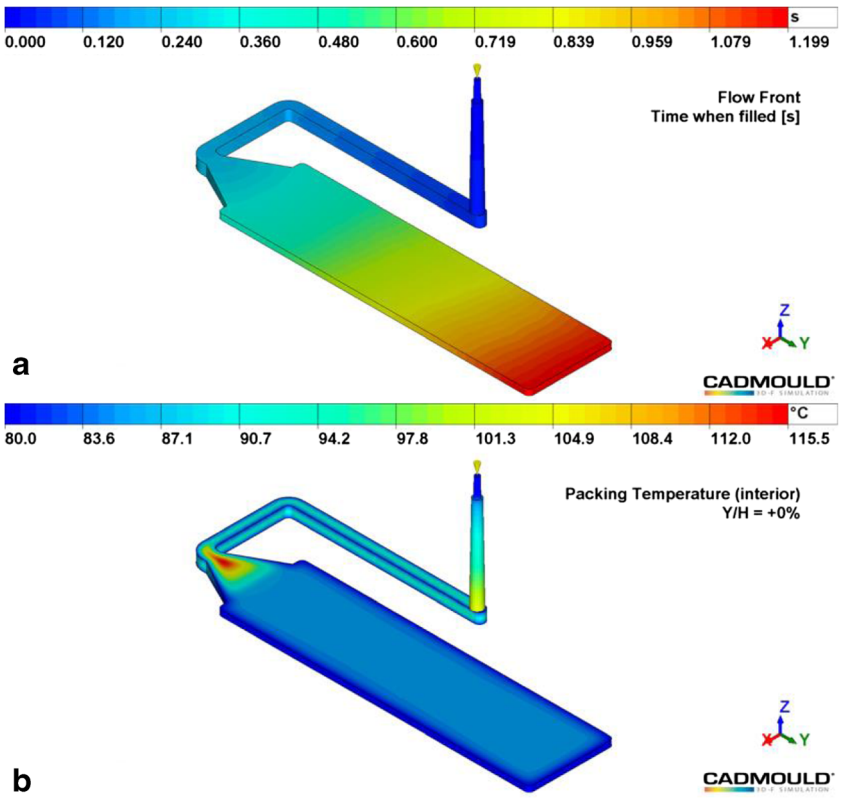

Fig. 3 Numerical simulation results of polyamide thermoplastic injection moulding. **a** Evolution of flow front during the filling stage. **b** The temperature distribution of the polyamide substrate at the end of the injection moulding process

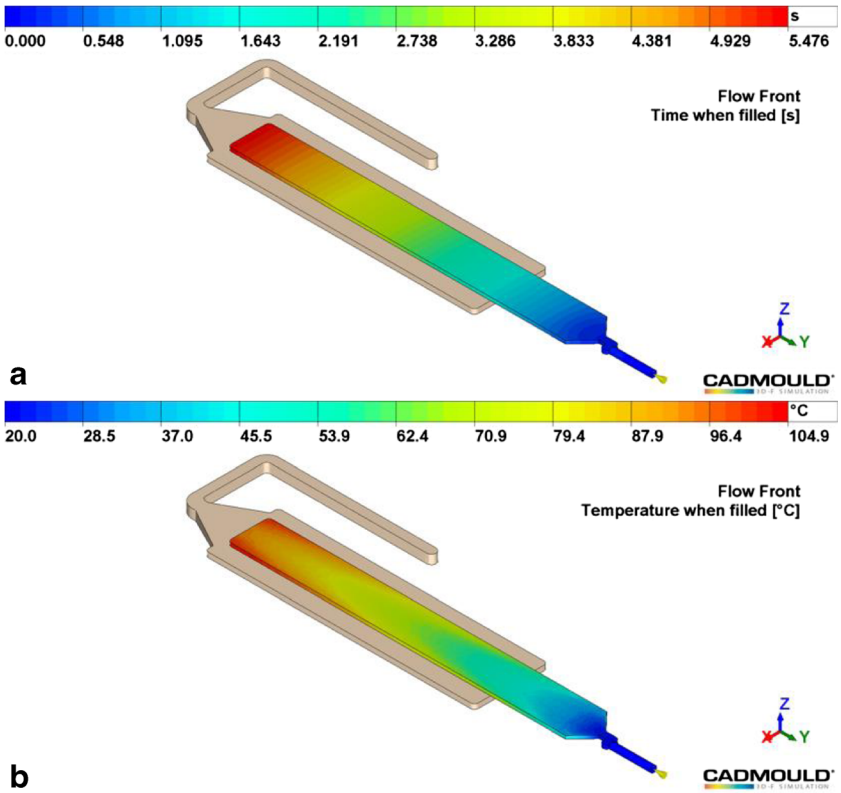

Fig. 4 Numerical simulation results of LSR injection moulding. **a** Evolution of flow front during the filling stage. **b** The temperature distribution of the LSR part at the end of the filling stage

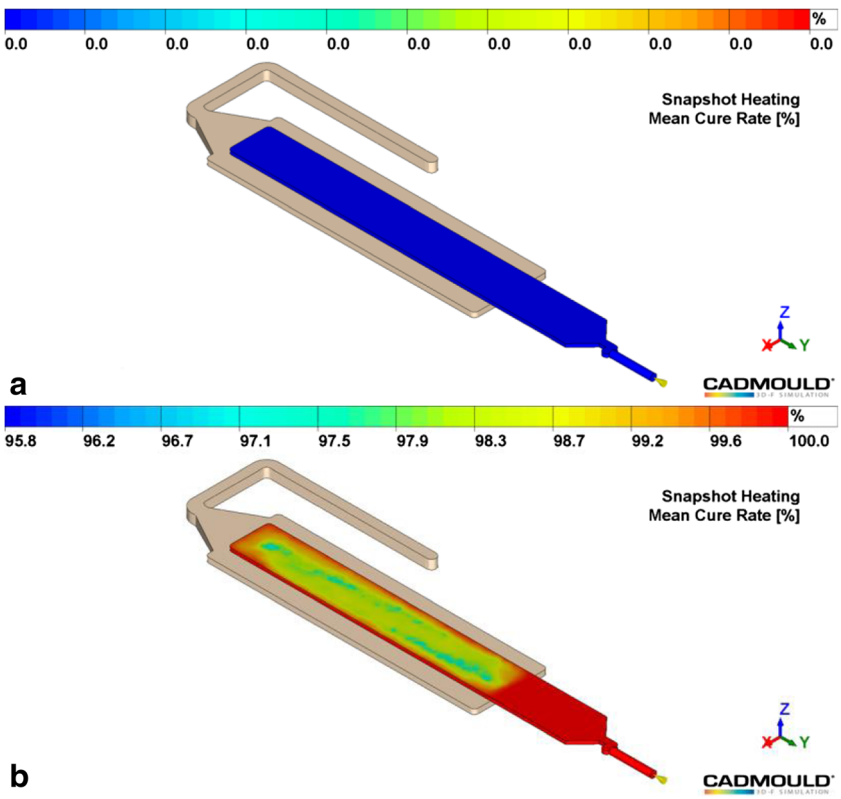

Fig. 5 Numerical simulation results of LSR injection moulding. **a** Cure degree at the end of the filling stage. **b** Cure degree at the end of the heating stage

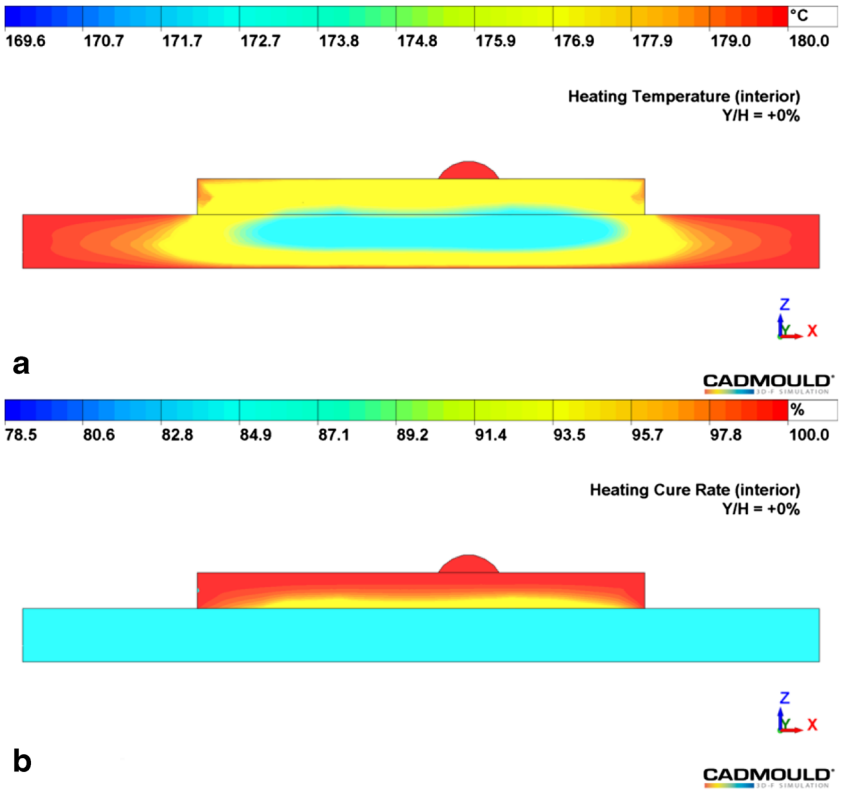

Fig. 6 Numerical simulation results of LSR injection moulding. **a** Temperature distribution. **b** Cure degree cutaway views in the middle of the thermoplastic/elastomer standard peel test specimen

increases very slowly (α remains close to zero), followed by the cure step, with a sharp increase of the elastic modulus (and α). During this step, the modulus increases up to a maximum value (G'_{max}) [30].

The kinetic model used for describing the curing reaction was proposed by Isayev and Deng, which is defined as [31].

$$\alpha = \frac{k(t-t_s)^n}{1 + k(t-t_s)^n} \tag{4}$$

where k, n and t_s are the rate constant, the order of reaction and the scorch time, respectively. In the elastomer industry, the scorch time (t_s) is usually defined as the time at which the cure degree is equal to 0.05. In this investigation, the scorch time was defined as the time when the value of the storage modulus was equal to that of loss modulus [32]. The rate constant depends on the temperature with an Arrhenius expression.

$$k = k_0 \exp\left(-\frac{E_0}{RT}\right) \tag{5}$$

where k_0, E_0, R and T are the pre-exponential factor of reaction velocity, the activation energy, the universal gas constant and the absolute temperature, respectively. In addition, the Claxton-Liska model was used to fit the scorch time (t_s), which is also expressed by an Arrhenius-type temperature dependence [27].

$$t_s = t_0 \exp\left(\frac{T_0}{T}\right) \tag{6}$$

where t_0 and T_0 are the material constants.

Table 2 Mechanical properties of LSRs and TCS used

Liquid silicone rubbers	Density (g cm^{-3})	Hardness shore A	Tensile strength (MPa)	Elongation at break (%)	Mix ratio A/B	
LSR4350	1.12	50	8.4	570	1:1	LSR4350A
						LSR4350B
LSR4370	1.14	68	9.0	450	1:1	LSR4370A
						LSR4370B
TCS7550	1.25	52	5.5	200	1:1	TCS7550A
						TCS7550B

Table 3 Mechanical and thermal properties of the polyamide thermoplastic material used

Polyamide PA 66	PA 66-GF 30
Density (g cm^{-3})	1.14
Tensile strength at break (MPa)	80
Young's modulus (MPa)	3200
Melting temperature	220
Thermal conductivity of melt (W mK^{-1})	0.183
Specific heat capacity of melt (J $(kg\ K^{-1})^{-1}$)	2700
Eff. thermal diffusivity ($m^2\ s^{-1}$)	7.10^{-8}
Ejection temperature (°C)	140

2.3 Fitting procedure

From the rheological measurements, the shear viscosities versus shear rate and temperature curves were fitted using the Carreau-Yasuda and WLF models, where the fitting parameters were determined by the inverse method. In addition, the constants of the Claxton-Liska and Isayev-Deng models were obtained by data fitting techniques and the inverse method using the curve fitting software Origin from the curing measurement experimental data.

Different identifications according to the inverse method were achieved by solving a minimization problem of the cost function using algorithms based on the generalized reduced gradient method:

$$\min_x \|F(x, x_{\text{data}}) - y_{\text{data}}\|_2^2 = \min_x \sum_i \left(F(x, x_{\text{data}} a_i - y_{\text{data}} a_i)\right)^2 \quad (7)$$

where y_{data} is the experimental data curve; x_{data} is the estimated value of the rheological or vulcanization behaviour model, according to variable values of the model parameters being optimized; $F(x, x_{\text{data}})$ is the rheological or curing model used; and x is the parameter to be identified.

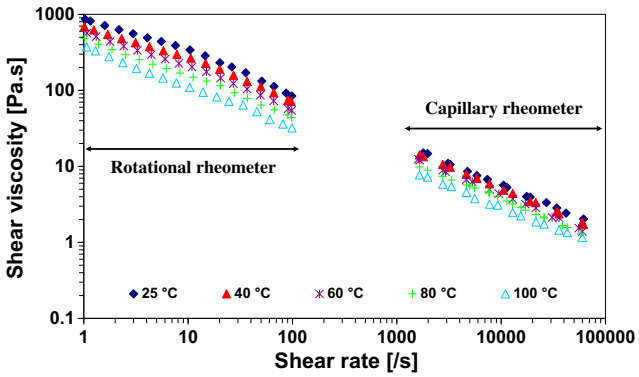

Fig. 7 Shear viscosity versus shear rate experimental curves include a large range of shear rates from 1 to 10^5 s^{-1} and 25 to 100 °C at different temperatures for the elastomer material LSR4350

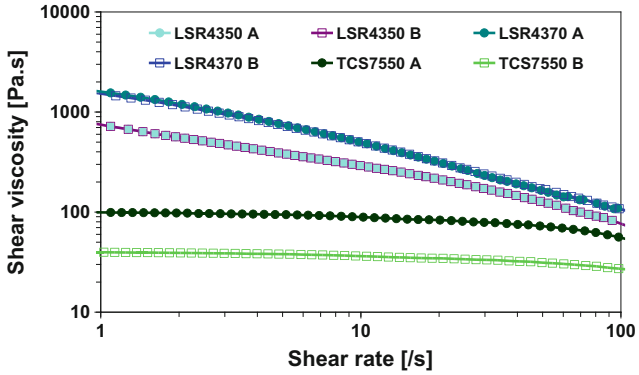

Fig. 8 Shear viscosity versus shear rate experimental curves obtained from 1 to 10^2 s^{-1} at room temperature for the different parts (A/B) of the materials studied

3 Numerical simulations

3.1 Boundary and initial conditions

Numerical simulation of polyamide thermoplastic polymer/LSR injection moulding was carried out with a polyamide thermoplastic polymer/rubber standard peel test specimen. The dimension of the standard peel test specimen is illustrated in Fig. 1. The numerical simulation of PA 66/LSR injection moulding was divided into two steps: first, the thermoplastic injection moulding of the polyamide substrate, and then, the over-moulding of LSR onto the surface of the polyamide substrate (Fig. 2). During the injection moulding process, the initial wall temperature of the mould was assumed to be constant, and gravity was also considered in the simulation, as shown in Table 1. In addition, the process parameters used in the simulation for polyamide thermoplastic injection moulding and LSR injection moulding are summarized in Table 1.

3.2 Numerical results and discussion

The first step of the numerical mould filling simulation of the injection, packing and cooling stages was realized with Cadmould® software and corresponded to the injection of the

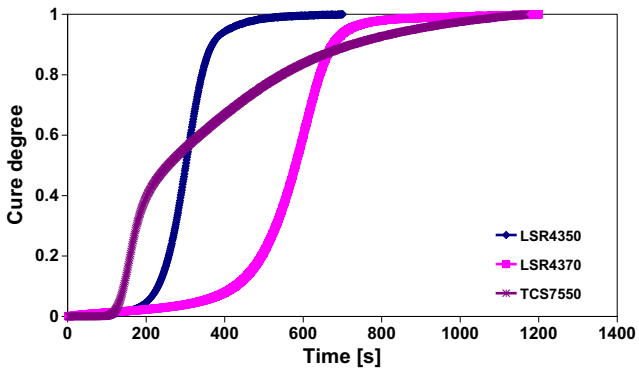

Fig. 9 Evolution of experimental cross-linking versus time at 100 °C using the M4350, M4370 and TCS7550 liquid silicone rubbers

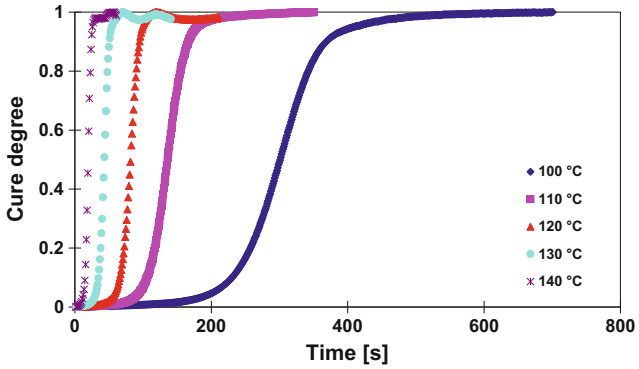

Fig. 10 Evolution of experimental cross-linking versus time and temperature for LSR4350

polyamide substrate. The mesh used is defined in Fig. 2a. The injection parameters used during simulation are defined in Table 1. The rheological and thermal parameters correspond to the data sheet of the PA 66-GF 30 polyamide provider. The numerical results of polyamide thermoplastic injection moulding are illustrated in Fig. 3a. It can be noted that the filling time was approximately 1.2 s for the full filling of the runner, gate and plate. The substrate presents a temperature approximately 80 °C after the cooling stage, and the maximal temperature of 115 °C is localized in the gate zone (see Fig. 3b). The temperature around the mould wall is approximately 85 °C.

In the second step of the numerical simulation, a two-component moulding filling simulation corresponding to the LSR over-moulding on a polyamide substrate plate (corresponding to a standard peel test specimen) was investigated. The runner and gate of this specific elastomer is located opposite the polymer plate. The injection parameters used are defined in Table 1. The rheological and cure kinetic parameters are in defined in Tables 4 and 5. The rheo-kinetics models used and the identified parameters were implemented in the Cadmould® software.

In addition, the temperature field of the polyamide substrate was implemented in the initial conditions for the simulation of LSR injection moulding. The evolution of the flow front during the filling stage of LSR injection moulding on a polymer substrate is illustrated in Fig. 4a. The filling time is approximately 5.48 s. During the injection, the elastomer material was heating by the polyamide substrate and the mould wall. It reached 104.9 °C at the end of the filling stage (Fig. 4b). The goal was to choose the proper injection conditions to avoid premature curing during filling, which could result in an incompletely filled part. There are a number of causes of this problem, such as slow filling, high mould surface temperature and so on. The evolution of the cure degree during injection moulding is illustrated in Fig. 5a. It shows that the cure degree at the end of the filling stage is almost zero and grows significantly during the heating stage (Fig. 6b). Moreover, the cure degree distribution demonstrates the effect of temperature on the kinetics of the cure reaction. It is of interest that the zone of the LSR part in contact with the die cavity mould walls present a greater cure degree (>99.6%) than that in contact with the polyamide substrate (~97.5% or more). A cutaway view of the temperature distribution in the middle of the thermoplastic/elastomer standard peel test specimen is shown in Fig. 6a. Because of the difference in thermal conductivity between the thermoplastic and die cavity mould materials, the temperature of the LSR part at the surface that is in contact with the mould wall is greater than that in contact with the substrate, resulting in faster kinetics of the cure reaction being observed at the exterior surface, as shown in Fig. 6b. This therefore shows that it is possible to simulate proper cavity filling and curing phases.

4 Materials and experimental techniques

4.1 Materials

The commercially available silicone reactants were kindly supplied by Bluestar Silicones as Silbione® two-part systems (LSR4350, LSR4370 and TCS7550). The LSR silicones used have specific properties: ultra-low durometer values, high performance (LSR4370), fast cure at elevated temperature, self-lubrication and over-moulding ability. The thermoplastic material PA 66-GF 30 used is a black polyamide PA 66 with a 30% glass filler. The main mechanical and thermal properties of these materials (LSRs, TCS and PA 66) are summarized in Tables 2 and 3.

4.2 Rheological and curing kinetic characterizations

The rheological measurements were carried out using a rotational HAAKE MARS III rheometer and a capillary Rosand

Table 4 Material constants for the Carreau-Yasuda model with the WLF equation

Material	T_0 (°C)	C_1	C_2 (°K)	$\eta_0(T_0)$ (Pa·s)	τ (Pa)	a	Number
LSR4350	25	4.30	428.92	3390.73	1940.72	0.39	0.35
LSR4370	25	70.80	6861.20	27,019.59	2139.14	0.28	0.27
TCS7550	25	3.08	304.24	76.28	11,789.00	0.76	0.34

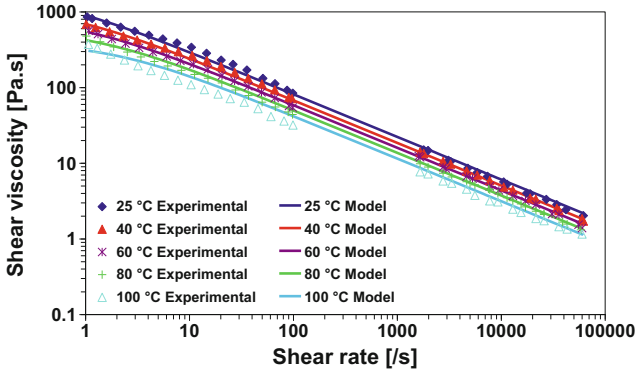

Fig. 11 Shear viscosity experimental results and Carreau-Yasuda model fitting curves at different temperatures for LSR4350

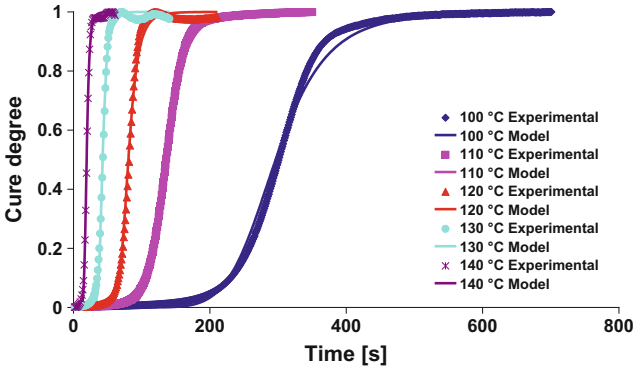

Fig. 13 Curing kinetic experimental results and Isayev-Deng model fitting curves at different temperatures for LSR4350

RH2000 rheometer for the mixture of liquid silicone rubber without a platinum catalyst as well as the two different parts (A/B) of the silicone elastomer at different temperatures from 25 to 100 °C. Characterization was carried out by a rotational rheometer that operates in a cone-and-plate geometry with a diameter of 35 mm and an angle of 2° over a shear rate ranging from 1 to 10^2 s^{-1}. Characterization by a capillary rheometer was carried out with a 0.5-mm-diameter die of 16 mm length over a shear rate ranging from 10^2 to 10^5 s^{-1}. The shear viscosity versus shear rate curve was recorded.

The curing measurement of liquid silicone rubber was carried out in dynamic mode using a rotational HAAKE MARS III rheometer operating in parallel-plate mode. The trays had a diameter of 20 mm and a thickness of 0.5 mm. The mixtures of the different elastomer materials were characterized for their cure characteristics using the mean of elastic modulus curves obtained under isothermal conditions. The test temperatures used were from 25 to 140 °C. The frequency used in the measurement was 1 Hz, with a deformation of 1%. The raw data obtained is complex torque (M^*), the real part of which G' is related to the storage modulus of the rubber. During the cure reaction, the values of the torque (M), storage modulus (G') and loss modulus (G'') were obtained during the curing measurement. These data were used to calculate the cure kinetic parameters.

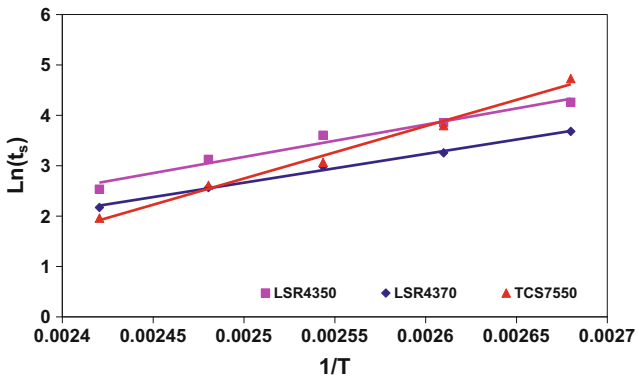

Fig. 12 Scorch times obtained at different temperatures with different systems according to the Claxton-Liska model

5 Experimental results and discussion

5.1 Rheometric tests

The shear viscosity versus shear rate curves obtained by the rotational rheometer and capillary rheometer at different temperatures for the mixture of silicone LSR4350 are shown in Fig. 7. The temperature ranges covered by the measurement were from 25 to 100 °C and include a large shear rate ranging from 1 to 10^5 s^{-1}. From the plots, it is clear that the shear viscosity decreases when either the temperature or shear rate increases, indicating a pseudoplastic flow behaviour. One can also observe that the differences between the experimental curves at different temperatures are relatively small at a high shear rate.

The curves of shear viscosity versus shear rate obtained by the rotational rheometer at room temperature for the different parts (A/B) of the materials studied are also shown in Fig. 8. Here, the A and B components were measured separately. It is worth noting that the two parts of LSR4350A and LSR4350B and LSR4370A and LSR4370B present the same rheological behaviour with the increasing shear rate, indicating a pseudoplastic flow behaviour from 1 to 10^2 s^{-1} at ambient temperature. The two parts of TCS7550A and TCS7550B nearly present as Newtonian fluids in the measurement interval from 1 to 10^2 s^{-1} at ambient temperature.

Table 5 Identified material constants of the Isayev-Deng model combined with the Claxton-Liska model for elastomer materials

Material	k_0 (s^{-1})	E_0 (kJ mol^{-1})	Number
LSR4350	exp(49.31)	178.63	2.15
LSR4370	exp(39.20)	148.34	2.06
TCS7550	exp(20.23)	80.23	1.21

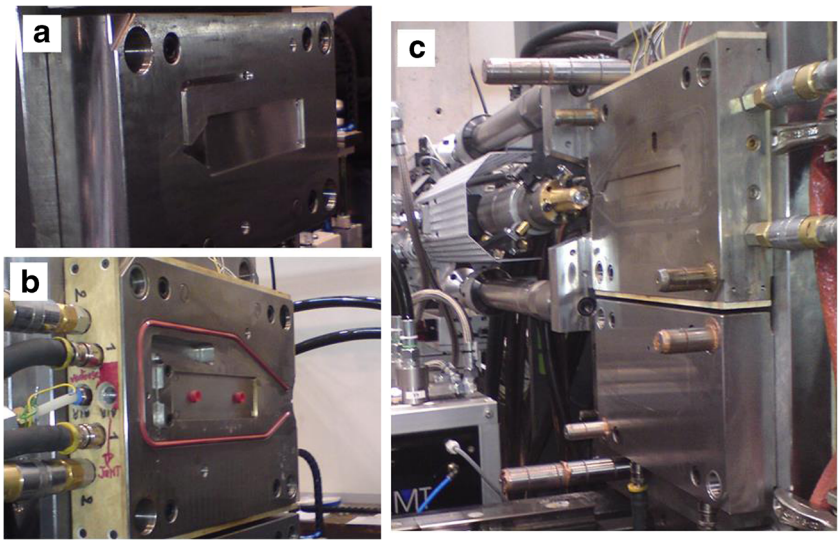

Fig. 14 **a** Die cavity for the injection of the thermoplastic substrate. **b** Die cavity for the insert of thermoplastic substrate. **c** Cavity for the over-moulding of liquid silicone rubber

5.2 Curing measurement

The cycle time is a very important parameter because a high cure time basically means lower profits. The cure time is the longest part of the cycle and is influenced by the choice of materials and their properties, as clearly shown in Figs. 5 and 6.

The curing kinetic curves obtained by the rotational rheometer at 100 °C for the three materials LSR4350, LSR4370 and TCS7550 are illustrated in Fig. 9. Here, the LSR is measured between two heated plates. It shows that the cure degree increases with increasing cure time and that the curves can be divided into three periods: induction, cure and reversion. During the induction period, the cure degree is nearly zero and increases slowly. Then, it grows rapidly toward one during the cure period.

The evolution of the cure degree with curing time obtained at different temperatures for the silicone elastomer LSR4350 is presented in Fig. 10. It can be observed that the cure degree increases with time under given isothermal conditions. Initially, the curing rate is low, but later, the reaction increases rapidly then gradually levels off, approaching a value of 1. Additionally, with a temperature increase from 100 to 140 °C, the cross-link density increases more rapidly and the plateau is reached in a shorter time.

5.3 Rheological and curing kinetic parameter identification

The Carreau-Yasuda model was fitted to the experimental results with a WLF-type temperature dependence. The reference temperature selected was 25 °C. The model parameter values resulting in the best fits to the experimental data for the Carreau-Yasuda model and WLF equation are listed in Table 4. The measured viscosity values and corresponding fitted viscosity curves for silicone LSR4350 are shown in Fig. 11. As can easily be observed, the rheological tests are in good agreement with the modelling under all of the different experimental conditions. It can be noted that a reasonable fit was obtained for the test temperatures over the shear rate ranges with the Carreau-Yasuda model.

After curve fitting using the inverse method with the Carreau-Yasuda model, the value of n varied from 0.28 to 0.76 for different elastomers, corresponding to a shear-thinning behaviour (see Table 4).

There are different definitions of the induction period or scorch time for elastomers. Consideration of the induction period, which is due to curing, is necessary to prevent any vulcanization reaction from taking place during the pouring stage of the casting process. The scorch times at each test temperature were measured as the time when the storage modulus is equal to the loss modulus, and the temperature dependence of the scorch time was fitted with the Claxon-Liska model. The scorch time obtained and the associated fitting curve are presented in Fig. 12.

The Isayev-Deng model was used to fit the experimental cure curves at different temperatures. The comparison of the experimental curing kinetic results and the Isayev-Deng model fitting curves is shown in Fig. 13 for LSR4350 at different temperatures. These data were fitted to the Isayev-Deng model by curve

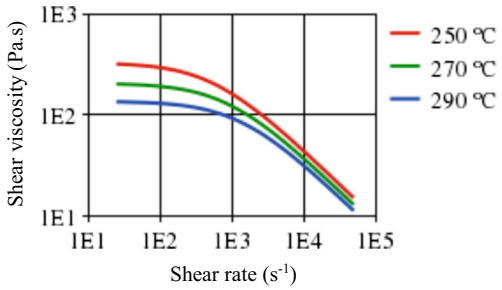

Fig. 15 Shear viscosity versus shear rate experimental curves of shear rates from 1 to 10^5 s^{-1} and 250 to 290 °C at different temperatures for PA 66 (GF 30)

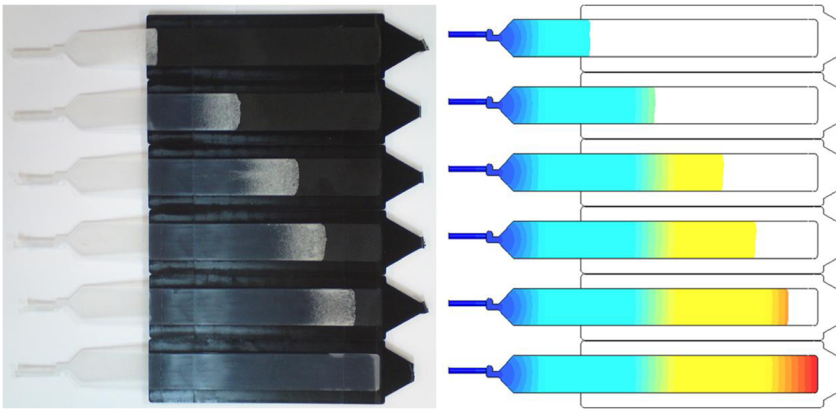

Fig. 16 Comparison between the flow front prediction and experimental results of liquid silicone rubber injected at different filling volumes made by bi-injection tests

fitting using an inverse method in Origin software, and the fitting of constant values together with the regression value is detailed in Table 5. The identified model is in very good agreement with the experimental results (gap <3%), although the model attains a total conversion faster than the experimental data for any of the temperatures. Despite this, the Isayev-Deng model presents an accurate description of silicone cross-linking for silicone LSR4350 at different temperatures. For example, after fitting the parameters for the LSR4350 elastomer compound, the activation energy of LSR4350 was 178.63 kJ mol^{-1}. For example, the full cure corresponding to LSR4350 silicone cross-linking was obtained with a long cure time (600 s) at an imposed temperature of 100 °C and a short cure time (45 s) for a temperature equal to 140 °C, as observed in Fig. 9. This S shape behaviour suggests that the reaction mechanism of vulcanization could be described by simple kinetic models. The data was fitted with the induction model proposed in the paper.

6 Experimental validation

In this investigation, bi-material injection moulding tests were performed with a thermoplastic injection moulding Billion Select 200T press coupled with an elastomer BOY injection external control unit. A special two-component mould that was used for the injection was designed and manufactured. The two-component mould comprises two parts. The lower part is the die cavity for the elaboration of the polyamide substrate, and the upper part is the die cavity for the over-moulding of LSR onto the thermoplastic substrate, as shown in Fig. 14.

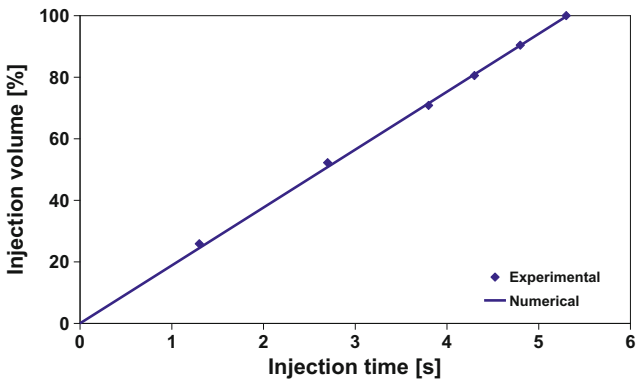

Fig. 17 Variation of injection volumes during the injection cycle obtained by experimental injection tests and numerical simulations

The injection tests were carried out with the same process conditions indicated in Table 1. The evolution of the flow front during LSR injection moulding was obtained by a series of tests carried out with different injection volumes. The curves of shear viscosity versus shear rate at different temperatures for the PA 66 are shown in Fig. 15. The temperature ranges covered by the measurement were from 250 to 290 °C and included a large shear rate ranging from 1 to 10^5 s^{-1}. From the plots, it is clear that the shear viscosity decreases when either the temperature or shear rate increases, indicating a pseudoplastic flow behaviour. To validate the model developed and parameters identified, a comparison of the flow front during the filling stage between the experimental and numerical results was performed. One of the aims of the simulations was to predict the flow front advancement to see how the mould fills, as shown in Fig. 16. The comparison of the flow front at different moments during injection tests shows that a good correlation is obtained between the experimental results and numerical simulations. The evolution of the injection volume during the bi-injection process and numerical results is shown in Fig. 17. The comparison shows good agreement, and there is a difference of less than 3%.

7 Conclusions

In this work, a thermo-rheo-kinetic model was developed for predicting the filling stage and curing stage of liquid silicone rubber during the injection moulding process. To identify the parameters of the model, the rheological and curing kinetic behaviour of silicone elastomer materials was investigated by a capillary rheometer and a rotational rheometer covering a large

shear rate. In addition, the thermo-physical properties of uncured and cured elastomer materials were measured by different associated methods. The numerical identification work shows that the Carreau-Yasuda model fits the shear viscosity behaviours of silicone LSR4350 well and the Isayev-Deng model also fits the curing kinetic reaction of elastomer materials well. The numerical simulation results present the evolution of the filling stage and the curing stage of LSR injection moulding, as well as the effect of the temperature distribution on the advancement of the cure degree inside the elastomer part. To validate the parameters identified and the numerical results obtained, a series of injection tests was carried out to compare the flow front of the elastomer materials during the filling stage, and a good correlation was obtained between the experimental and numerical results.

Acknowledgements The authors thank the collaborative FUI Project LSR Silicone and the IPC Center to have performed some injected components.

Compliance with ethical standards

Conflict of interest The authors declare that they have no competing interests.

References

1. Seyedmehdi SA, Zhang H, Zhu J (2012) Superhydrophobic RTV silicone rubber insulator coatings. Appl Surf Sci 258:2972–2976
2. Yan F, Zhang X, Liu F, Li X, Zhang Z (2015) Adjusting the properties of silicone rubber filled with nanosilica by changing the surface organic groups of nanosilica. Compos Part B 75:47–52
3. Chen D, Liu Y, Huang C (2012) Synergistic effect between POSS and fumed silica on thermal stabilities and mechanical properties of room temperature vulcanized (RTV) silicone rubbers. Polym Degrad Stab 97:308–315
4. Shang S, Gan L, Yuen MC, Jiang SX, Luo NM (2014) Carbon nanotubes based high temperature vulcanized silicone rubber nanocomposite with excellent elasticity and electrical properties. Compos Part A 66:135–141
5. Rey T, Le Cam JB, Chagnon G, Favier D, Rebouah M, Razan F, Robin E, Didier P, Heller L, Faure S, Janouchova K (2014) An original architectured NiTi silicone rubber structure for biomedical applications. Mater Sci Eng C 45:184–190
6. Doyle BJ, Corbett TJ, Cloonan AJ, O'Donnell MR, Walsh MT, Vorp DA, McGloughlin TM (2009) Experimental modelling of aortic aneurysms: novel applications of silicone rubbers. Med Eng Phys 31:1002–1012
7. Wang HS, Wang YN, Wang YC (2013) Cost estimation of plastic injection moulding parts through integration of PSO and BP neural network. Expert Syst Appl 40:418–428
8. Wang X, Xia Z, Yuan B, Zhou H, Li Z, Chen N (2013) Effect of curing temperature on the properties of conductive silicone rubber filled with carbonyl permalloy powder. Mater Des 51:287–292
9. Diao S, Dong F, Meng J, Ma P, Zhao Y, Feng S (2015) Preparation and properties of heat-curable silicone rubber through chloropropyl/amine crosslinking reactions. Mater Chem Phys 153:161–167
10. Fang W, Zeng X, Lai X, Li H, Chen W, Zhang Y (2015) Thermal degradation mechanism of addition-cure liquid silicone rubber with urea-containing silane. Thermochim Acta 605:28–36
11. Van der Houwen EB, Kuiper LH, Burgerhof JGM, Van der Laan BFAM, Verkerke GJ (2013) Functional buckling behavior of silicone rubber shells for biomedical use. J Mech Behav Biomed Mater 28:47–54
12. Rey T, Chagnon G, Le Cam JB, Favier D (2013) Influence of the temperature on the mechanical behaviour of filled and unfilled silicone rubbers. Polym Test 32:492–501
13. Kuo CC, Siao YT (2014) Measuring the solidification time of silicone rubber using optical inspection technology. Optik 125:196–199
14. Haberstroh E, Ronnewinkel C (2001) LSR thermoplastic combination parts in two-component injection moulding. J Polym Eng 21: 303–318
15. Nguyen S, Perez CJ, Desimone M, Pastor JM, Tomba JP, Carella JM (2013) Adhesion control for injection overmoulding of elastomeric propylene copolymers on polypropylene. Effects of block and random microstructures. Int J Adhes Adhes 46:44–55
16. Arzondo LM, Pino N, Carella JM, Pastor JM, Merino JC, Póveda J, Alonso C (2004) Sequential injection overmoulding of an elastomeric ethylene-octene copolymer on a polypropylene homopolymer core. Polym Eng Sci 44:2110–2116
17. Ansarifar MA, Chong LK, Zhang J, Bell A, Ellis RJ (2003) Effect of bifunctional organosilane on the joint strength of some natural rubber compounds to nylon 6,6. Int J Adhes Adhes 23:177–188
18. Zhang S, Dubay R, Charest M (2015) A principal component analysis model-based predictive controller for controlling part warpage in plastic injection molding. Expert Syst Appl 42:2919–2927
19. Wang Y, Yu KM, Wang CCL (2015) Spiral and conformal cooling in plastic injection moulding. Comput Aided Des 63:1–11
20. Dang XP (2014) General frameworks for optimization of plastic injection molding process parameters. Simul Model Pract Theory 41:15–27
21. Souid A, Sarda A, Deterre R, Leroy E (2015) Influence of reversion on adhesion in the rubber-to-metal vulcanization-bonding process. Polym Test 41:157–162
22. Aho J, Syrjälä S (2008) On the measurement and modelling of viscosity of polymers at low temperatures. Polym Test 27:35–40
23. Williams ML, Landel RF, Ferry JD (1955) The temperature dependence of relaxation mechanisms in amorphous polymers and other glass forming liquids. J Am Chem Soc 77:3701–3707
24. Bideau PL, Ploteau JP, Dutournié P, Glouannec P (2009) Experimental and modelling study of superficial elastomer vulcanization by short wave infrared radiation. Int J Therm Sci 48:573–582
25. Khang TH, Ariff ZM (2012) Vulcanization kinetics study of natural rubber compounds having different formulation variables. J Therm Anal Calorim 109:1545–1533
26. Wang J, Fang X, Wu M, He X, Liu W, Shen X (2011) Synthesis, curing kinetics and thermal properties of bisphenol-AP-based benzoxazine. Eur Polym J 47:2158–2168
27. Claxton WE, Liska JW (1964) Calculation of state of cure in rubber under variable time-temperature conditions. Rubber Age 95:237
28. Kamal MR, Sourour S (1973) Kinetics and thermal characterisation of thermoset cure. Polym Eng Sci 13:59
29. Isayev AI, Deng JS (1988) Non isothermal vulcanisation of rubber compounds. Rubber Chem Technol 61:340
30. Leroy E, Souid A, Sarda A, Deterre R (2013) A knowledge based approach for elastomer cure kinetic parameters estimation. Polym Test 32:9–14
31. Isayev AI, Deng JS (1987) Non isothermal vulcanisation of rubber compounds. ACS Rubber Division Meeting, Montreal, Canada
32. Souid A, Sarda A, Deterre R, Leroy E (2014) Rheological characterization and modelling of the rubber to metal vulcanization-bonding process. Polym Test 36:88–94